Math. Model. Nat. Phenom.
Vol. 9, No. 1, 2014, pp. 27–38
DOI: 10.1051/mmnp/20149103

A Fluid-Structure Interaction Model of the Cell Membrane Deformation: Formation of a Filopodium

N. El Khatib*

Department of Computer Science and Mathematics
Lebanese American University - Byblos campus, P.O. Box: 36, Byblos, Lebanon

Abstract. In this paper we present a fluid-structure interaction model of neuron's membrane deformation. The membrane-actin is considered as an elastic solid layer, while the cytoplasm is considered as a viscous fluid one. The membrane-actin layer is governed by elasticity equations while the cytoplasm is described by the Navier-Stokes equations. At the interface between the cytoplasm and the membrane we consider a match between the solid velocity displacement and the fluid velocity as well as the mechanical equilibrium. The membrane, which faces the extracellular medium, is free to move. This will change the geometry in time. To take into account the deformation of the initial configuration, we use the Arbitrary Lagrangian Eulerian method in order to take into account the mesh displacement. The numerical simulations, show the emergence of a filopodium, a typical structure in cells undergoing deformation.

Keywords and phrases: partial differential equations, cell membrane, fluid-structure interaction, numerical simulations

Mathematics Subject Classification: 35Q30, 92C50, 74F10

1. Introduction

The cell membrane is a biological membrane that separates the intracellular environment from the extracellular one [1]. It basically protects the cell from outside forces. Cell membranes are involved in a variety of cellular processes such as cell adhesion and motion. On December 29, 2011, chemists at Harvard University reported the creation of an artificial cell membrane [3].

The cell membrane consists primarily of a thin layer of phospholipids (see Figure 1(a)) which spontaneously arrange so that the hydrophobic *tail* regions are isolated from the surrounding polar fluid, causing the more hydrophilic *head* regions to associate with the intracellular and extracellular faces of the resulting bilayer. Hydrophobic interactions are the major driving force in the formation of lipid bilayers.

During development, motion [2] and differentiation, cell shape changes combining the production of internal forces at the molecular level. Actin (de)polymerization plays a key role in intracellular force generation [5, 16]. However the polymerization kinetics alone cannot account for a localized force, both in space and direction. This complex process is under the control of actin filament elongation from

*Corresponding author. E-mail: nader.elkhatib@lau.edu.lb

nucleation sites newly created at the membrane in response to extracellular signals and their assembly into the cell cytoskeleton by binding protein complexes. Hence, the amplitude and direction of the force is determined by the density of cytoskeleton and the macroscopic orientation of the actin filaments in contact with the membrane.

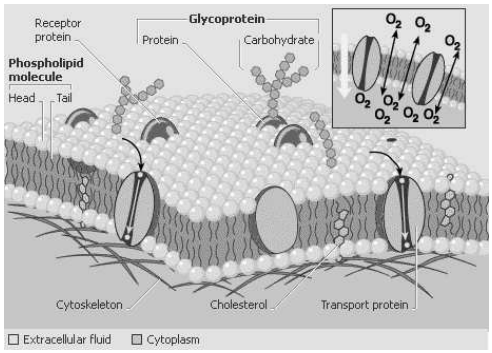

(a) Schematic of the membrane layers.

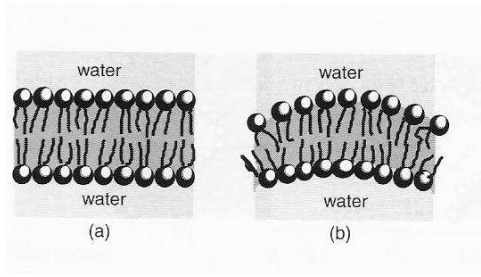

(b) Deformation of the membrane bilayer.

FIGURE 1. Membrane deformation

At the growing end of the filaments, the association of actin monomers produces work directed against the membrane and is responsible of a net displacement of the membrane (see figure 2(a)).

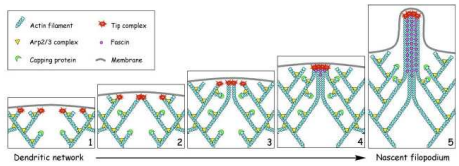

(a) Organization of the actin cytoskeleton during the filopodium formation. (Adapted from [17])

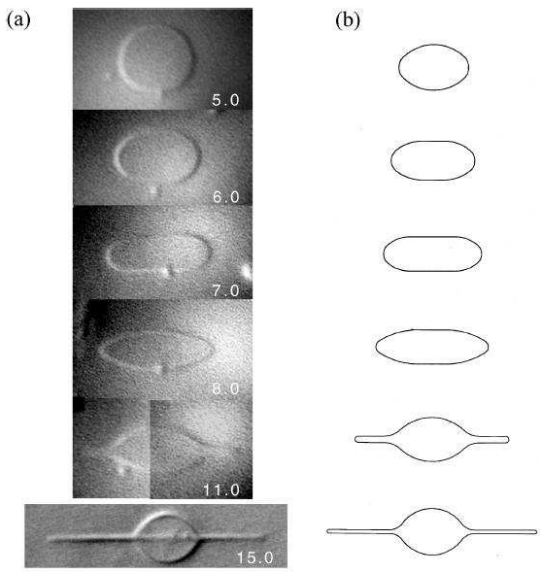

(b) Formation of the filopodium.

FIGURE 2. Filopodium formation.

In the literature, several models have been proposed. In [6] the author proposed a model without considering the membrane's thickness so that this membrane can be considered as a free boundary submitted to the action of the cytoplasm (fluid). Other models incorporate the chemical activity of monomer aggregation and the filament mechanical properties [9,13,14]. In all these modeling approaches, actin filaments exert their force against a purely passive membrane, without mechanical resistance to shear (extension) or bending of the latter. However, experimental studies, using different techniques and biological material, have shown the importance of the whole cell during deformation [8, 10, 11, 15, 18]. From these results, two issues raise. First, the cell interface, which spans the lipid bilayer and the cell cortex, is complex and can respond to stimulation by modifying its mechanical behavior, either because the microscopic cytoskeleton structure changes or because membrane effective area is expanded during filopodia extension (see Figure 2(b)). Second, cell protrusions, such as filopodia, represent long deformations, with a narrow base spanning at most a few tenth of a micrometer. Therefore, during the emergence of the filopodium the rest of the cell body stays immobile and exerts a no-displacement constraint at the filopodium base that modifies the final equilibrium configuration of the membrane.

To study and analyze these issues, we model the emergence of thin structures (filopodium like) driven by a localized internal force, mimicking newly synthesized actin filaments at the cell interface. A first attempt to model the membrane deformation using this approach was proposed in [7]. In this approach we take into account the membrane reaction to intracellular forces as well as the convection of cytoplasm in response to membrane displacement. To keep the complexity of the model at an acceptable level, we just consider the complex membrane-actin cortex as an elastic shell with elastic properties. The force field, which is related to the actin polymerization activity in the cytoplasm, is given as a function of position and time, with a characteristic length-scale of one tenth of micrometer. Additionally, we assume that the pushing activity peaks 20 seconds after the activity onset and decreases over 20 seconds after saturating during the same period.

We show that the membrane can resist forces from the cytoplasm over large intervals for the tension and bending parameters by producing broad and shallow membrane bending. However, allowing the membrane mechanical characteristics to vary with the membrane composition and the dynamics of the force, yields a long and thin protrusion, resembling a nascent filopodium.

The model we suggest in this study is a simplified one that considers the membrane as an elastic layer submitted to a mechanical force produced by the cytoplasm considered as a fluid. The employment of the Arbitrary Lagrangian-Eulerian method is the numerical tool that allows us to couple the fluid and solid equations.

2. Model and equations

The structure of cells and their membrane is complex (see Figures 1) and its representation should be simplified before the modeling step itself. The modeled section of the cell is shown in Figure 3.

Although discrete elements can be identified at the cell periphery (membrane and the cortex, a densely packed mesh of cross-linked actin filaments) or in the cytoplasm (cell nucleus, actin cables, tubulin filaments), we adapt our description at a mesoscopic level, between the molecular level and the whole cell. Basically, the membrane and the actin cortex are tightly coupled so that we can consider them as a unique structure with elastic properties (Navier equations). The cytoplasm is a mixture of water, ions, proteins and organites. In our approach, we model it as a highly viscous fluid (Navier-Stokes equations). Finally, since we couple Eulerian (Navier-Stokes) and Lagrangian (Navier) variables, we also included an application to account for the coupling of the velocity field (Navier-Stokes equations) with the time variation of the displacement (Navier equations) and the displacement of the mesh.

We consider a rectangular domain Ω that represents a 2D slice of an actual cell. The dimensions of Ω are representative of a typical motile cell, such a fibroblast or a leucocyte. The total domain Ω is divided into two sub-domains Ω_s (membrane and actin cortex) and Ω_f (cytoplasm) (see Figure 4). All equations will be expressed in the actual deformed configuration Ω_s or Ω_f. In Ω_s, we impose that the material

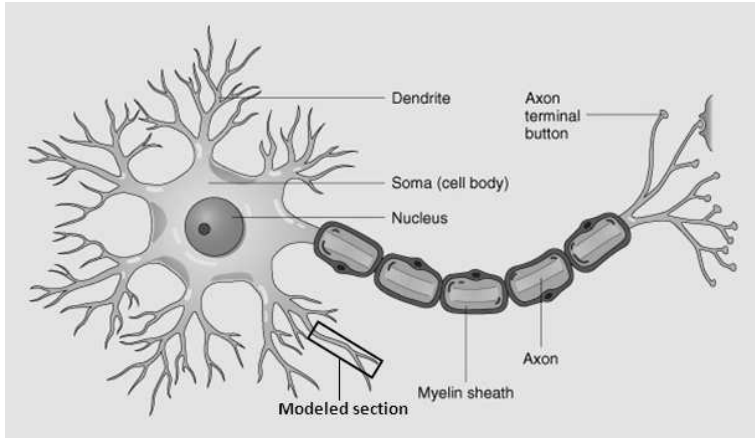

FIGURE 3. Modeled section of the neuron

displacement, $\mathbf{W}$, should be solution of the elasticity equations given by

$$\rho_s \frac{\partial^2 \mathbf{W}}{\partial t^2} = \nabla . \mathbf{P}_s, \tag{2.1}$$

where

$$\mathbf{P}_s = \lambda \, \mathrm{tr}(\mathbf{E}) \mathbf{I} + 2\mu \mathbf{E},$$

where λ and μ are the Lamé cœfficients, ρ_s is the solid mass density and $\mathbf{E}$ is the Green tensor that verifies

$$2\mathbf{E} = \nabla \mathbf{W} + \nabla \mathbf{W}^T.$$

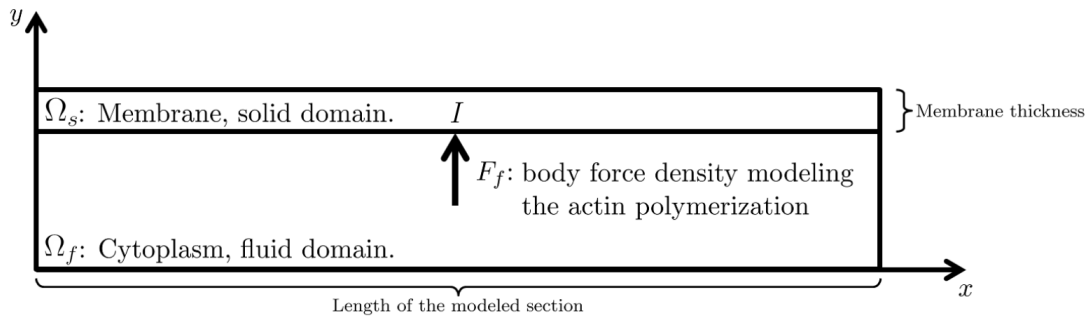

FIGURE 4. Schematic representation of the modeled section.

In the second sub-domain Ω_f, we solve the Navier-Stokes equations for the cytoplasm:

$$\begin{cases} \rho_f \left(\dfrac{\partial \mathbf{u}}{\partial t} + \mathbf{u} . \nabla \mathbf{u} \right) + \nabla p = \nabla . \boldsymbol{\sigma}_f + \mathbf{F}_f \\ \nabla . \mathbf{u} = 0 \end{cases} \tag{2.2}$$

with ρ_f as the fluid density, p the pressure and $\mathbf{F}_f$ the body force density. The stress tensor is given by:

$$\boldsymbol{\sigma}_f = 2\eta(\nabla \mathbf{u} + \nabla \mathbf{u}^t),$$

where η is the fluid viscosity coefficient. On immobile boundaries of Ω (boundaries 1, 2, 3 and their symmetric part), we impose a zero velocity (sub-domain Ω_f) or a zero displacement (sub-domain Ω_s). The upper boundary of Ω_s which corresponds to the membrane facing the extracellular medium, is free to move. Hence, we impose that the normal and tangent components of the stress vanish

$$\mathbf{P}_s = 0.$$

Actin polymerization, which generates the mechanical force at the molecular level, is encoded into the body force ($\mathbf{F}_f$ in the right hand side of the equation in Ω_f). Because of the mesoscopic level adopted throughout this paper, the actin force is equivalent to

$$\mathbf{F}_f = A\mathbf{n},$$

with a space and time dependent amplitude A and a direction given by the unit vector $\mathbf{n}$. In the simulation, we used a vertically oriented force, in Ω_f, centered at $I(x_I, y_I)$ and formulated as

$$A(t, x, y) = e^{-(x-x_I)^2-(y-y_I)^2} \frac{t}{t+1}$$

where $e^{-(x-x_I)^2-(y-y_I)^2}$ models the force amplitude with a gaussian behavior centered at the point I. The fraction $\dfrac{t}{t+1}$ models the saturation of the force with time.

3. Coupling the fluid and the structure

We denote by Ω_f and Ω_s respectively, the solid and the fluid domain, and Γ^t the interface between these two domains (see Figure 5). This interface varies in time.

The fluid-structure interaction (FSI) problem results from coupling the fluid equations (2.2) with the structure equations (2.1). The coupling occurs at the interface Γ^t, through the matching conditions between the solid and the fluid, given by

$$\mathbf{u} = \frac{\partial \mathbf{W}}{\partial t} \quad \text{on } \Gamma^t. \tag{3.1}$$

$$-\boldsymbol{\sigma}_f \mathbf{n} + \mathbf{P}_s \mathbf{n} = 0 \quad \text{on } \Gamma^t. \tag{3.2}$$

where $\mathbf{n}$ is the normal unit vector to Γ^t. Condition (3.1) is the no-slip condition, that guarantees the total adherence of the fluid to the structure, while (3.2) establishes the continuity of the stresses. The

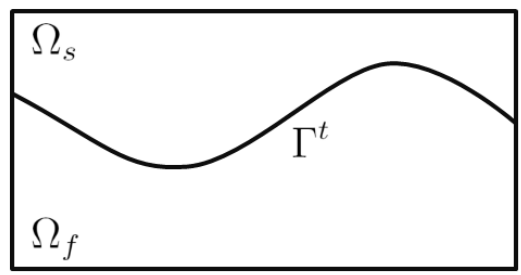

FIGURE 5. Boundary conditions on the interface

left, right and bottom boundaries are considered as fixed boundaries ; whereas the top boundary of the solid domain is set to be free boundary.

3.1. Moving mesh: ALE formulation

One of the difficulties in dealing with fluid-structure interaction (FSI) is the relation between Lagrangian and Eulerian descriptions. Solid dynamics is more naturally described in terms of reference configuration and deformation function (Lagrangian description) whereas fluid equations are more easily expressed in terms of space coordinates in a fixed referential (Eulerian description). The choice of the Arbitrary Lagrangian Eulerian (ALE) formulation is to use a Lagrangian framework for the solid and a mixed formulation for the fluid: the time derivatives are expressed as functions of the Lagrangian reference coordinates, whereas the space derivatives are left expressed as functions of the fixed Eulerian coordinates, since their expression is much simpler. The Lagrangian formulation of the time derivatives involves the domain velocity, which is the time derivative of the deformation function, and is often called *mesh velocity* since it gives the velocity of each mesh node in the fixed referential.

We refer to [19, 20, 25] for a detailed description and study of the ALE method.

In order to adapt the mesh with the motion, we rewrite the equations of a mobile domain. This will lead to the formulation known as the Arbitrary Lagrangian Eulerian (ALE) formulation. For that, we define a mapping from the initial configuration to the mobile configuration.

Let $\Omega_0 \subset \mathbb{R}^2$ be the initial domain (at $t = t_0$), $\Omega_t \subset \mathbb{R}^2$ be the domain at a point of time t and $\mathcal{A}_t$ be a set of mappings that associate at any point of time $t \in (t_0, T)$ a point Y in Ω_0 to a point x in Ω^t.
One can say that, $\forall t \in (t_0, T)$:

$$\mathcal{A}_t : \Omega_0 \subset \mathbb{R}^2 \to \Omega^t \subset \mathbb{R}^2, \qquad x(Y,t) = \mathcal{A}_t(Y)$$

Denote by I the interval (t_0, T).
We call $Y \in \Omega_0$ the *ALE coordinate* and $x = x(Y,t)$ the spatial coordinate (Eulerian).
Let $f : \Omega^t \times I \to \mathbb{R}$ be a function defined over the Eulerian domain and $\hat{f} := f \circ \mathcal{A}_t$ the corresponding function in the ALE domain, defined by:

$$\hat{f} : \Omega_0 \times I \to \mathbb{R}, \qquad \hat{f}(Y,t) = f(\mathcal{A}_t(Y), t)$$

We denote by $\left.\frac{\partial f}{\partial t}\right|_Y$ the derivative, with respect to time, in the ALE configuration, written with respect to spacial coordinates. It is defined by:

$$\left.\frac{\partial f}{\partial t}\right|_Y : \Omega^t \times I \to \mathbb{R}, \qquad \left.\frac{\partial f}{\partial t}\right|_Y (x,t) = \frac{\partial \hat{f}}{\partial t}(Y,t), \qquad Y = \mathcal{A}_t^{-1}(x) \tag{3.3}$$

Denote by $\left.\frac{\partial f}{\partial t}\right|_x$ the partial derivative with respect to time in the spacial configuration. We can write:

$$\left.\frac{\partial f}{\partial t}\right|_Y = \left.\frac{\partial f}{\partial t}\right|_x + \left.\frac{\partial x}{\partial t}\right|_Y \cdot \nabla_x f = \left.\frac{\partial f}{\partial t}\right|_x + \mathbf{\Psi} \cdot \nabla_x f.$$

Then, we define $\mathbf{\Psi}$, the domain's velocity with:

$$\mathbf{\Psi}(x,t) = \left.\frac{\partial x}{\partial t}\right|_Y \tag{3.4}$$

Now, we consider the general problem

$$\left.\frac{\partial \mathbf{u}}{\partial t}\right|_x + \mathcal{L}(\mathbf{u}) = 0 \tag{3.5}$$

where $\mathbf{u} = \mathbf{u}(x,t)$ ($x \in \Omega^t$ and $t \in I$) with the adequate boundary conditions.

$\mathcal{L}$ is a differential operator which can be linear or non-linear in the variable space x. Hence we obtain the following equation for $\mathbf{u} \circ \mathcal{A}_t$:

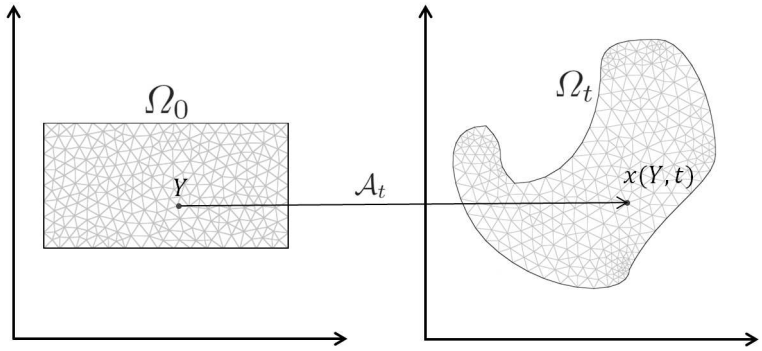

FIGURE 6. The geometry of the domain changes in time. The choice of the ALE formulation is to use a Lagrangian framework for the solid and a mixed formulation for the fluid: the time derivatives are expressed as functions of the Lagrangian reference coordinates, whereas the space derivatives are left expressed as functions of the fixed Eulerian coordinates.

$$\frac{\partial \mathbf{u}}{\partial t}\Big|_Y = \frac{\partial \mathbf{u}}{\partial t}\Big|_x + \frac{\partial x}{\partial t}\Big|_Y \cdot \nabla_x \mathbf{u} = \frac{\partial \mathbf{u}}{\partial t}\Big|_x + \mathbf{\Psi} \cdot \nabla_x \mathbf{u}. \tag{3.6}$$

where ∇_x is the gradient with respect to the variable x.

If we replace the last result in the equation (3.5), we obtain

$$\frac{\partial \mathbf{u}}{\partial t}\Big|_Y + \mathcal{L}(\mathbf{u}) - \mathbf{\Psi} \cdot \nabla_x \mathbf{u} = 0 \tag{3.7}$$

We call this formulation the ALE equivalent formulation of (3.5).

Hence if we apply the method described above on the fluid equations we get

$$\begin{aligned} \rho_f \frac{\partial \mathbf{u}}{\partial t} - \nabla \cdot [(-p)I + \eta(\nabla \mathbf{u} + (\nabla \mathbf{u})^T] + \rho_f((\mathbf{u} - \mathbf{\Psi}) \cdot \nabla)\mathbf{u} = 0 \qquad & in\ \Omega^t \\ \nabla \cdot \mathbf{u} = 0 & \end{aligned} \tag{3.8}$$

The ALE formulation of the quasi-Newtonian equation for fluids is then

$$\rho_f \left(\frac{\partial \mathbf{u}}{\partial t}\Big|_Y + (\mathbf{u} - \mathbf{\Psi}).\nabla_x \mathbf{u} \right) + \nabla_x p \quad = \quad \nabla_x . \boldsymbol{\sigma_f}$$

where Y is the Lagrangian coordinate, x the Eulerian coordinate and $\mathbf{\Psi}$ the mesh velocity.

Hence the fluid equations take into account the mesh motion during time, by adding the mesh velocity to the fluid flow velocity.

3.2. An energy estimate

Here we present an energy estimate for the FSI coupling problem. The FSI problem is highly nonlinear since the solution for the fluid equations depends on the domain Ω^t, which is variable in time, depending on the solution $\mathbf{W}$ of the structure equations. Moreover, the solution of the structure equations depends itself on the fluid load on the membrane, that is, on the fluid solution. This complexity of the FSI problem makes it difficult to obtain regularity results for the coupled problem, as well as to study its well-posedness. Precisely, the 2D elastic model does not provide a priori sufficient regularity of the solution $\mathbf{W}$ for the coupling with the fluid equations. Indeed, from the matching conditions (3.1)-(3.2),

we see that the fluid velocity at the interface boundary Γ^t with the structure wall is given by the time derivative of the wall displacement $\dot{\mathbf{W}}$, which does not, in general, belong to $H^{1/2}(\Gamma^t)$, that is the natural space for the trace of the fluid solution $\mathbf{u}(t) \in H^1(\Gamma^t)$.
In the literature, several authors add extra regularizing terms to the structure model, in search of regularity results for the FSI problem, that however do not have a direct physical or biological meaning [22, 23]. We refer to [20, 24], for more recent results for strong solutions of the FSI problem using 3**D** elasticity structure models, after reducing the case to the 2**D** one.

Due to these difficulties, we assume a priori some regularity hypothesis, so that the integral and norms used to derive the stability result are well defined. In particular, we assume that $\mathbf{u}(t) \in H^1(\Gamma^t)$, and also that $\dot{\mathbf{W}} \in H^{1/2}(\Gamma^t)$, which guarantees that $\mathbf{u}(t) \in H^1(\Omega^t)$. Moreover, since the fluid domain Ω^t depends on the structure model solution, we assume that such solution is regular enough so that Ω^t is sufficiently regular at all times. In particular, we consider that, at any time t the domain $\Omega^t \in \mathbb{R}^2$ is open and connected and its boundary $\partial\Omega^t \in \mathcal{C}^{1,1}$.

In [21] authors formulated an estimate for the energy of the coupled FSI problem (2.2), (2.1), (3.2), (3.1) defined as

$$\mathcal{E}(t) = \frac{\rho_f}{2}\|\mathbf{u}\|^2_{L^2(\Omega^t)} + \frac{\rho_s}{2}\|\dot{\mathbf{W}}\|^2_{L^2(\Gamma(0))} + \mu\|\mathbf{E}\|^2_{L^2(\Gamma(0))} + \frac{\lambda}{2}\|\mathrm{tr}\mathbf{E}\|^2_{L^2(\Gamma(0))}.$$

Theorem 3.1. *The coupled FSI problem (2.2), (2.1), (3.2) and (3.1), with homogeneous Dirichlet boundary conditions $\mathbf{u} = 0$ on $\Gamma_l(t)$, $\Gamma_r(t)$ and $\Gamma_b(t)$, satisfies the following energy inequality:*

$$\frac{d}{dt}(\mathcal{E}(t)) + 2\eta\|\mathbf{D}(\mathbf{u})\|^2_{L^2(\Gamma^t)} \leq 0, \tag{3.9}$$

from which we obtain the energy decay property

$$\mathcal{E}(t) + 2\eta\int_0^t \|\mathbf{D}(\mathbf{u})\|^2_{L^2(\Omega^t)}\, dt \leq \mathcal{E}(0). \tag{3.10}$$

Proof. See theorem 3.9 in [21]. □

4. The numerical methods

A splitting strategy is used in order to perform the numerical approximation of the FSI coupling problem [26]. The solving algorithm operates as follows
Given a time step Δt

1. solve the system of equations in the fixed geometry,
2. update the geometry in function of the displacement in order to create the new geometry,
3. interpolate the variables values on the new geometry,
4. update and compute the boundary variables,
5. increase the time step and redo the loop.

This corresponds to an Euler explicit scheme in time.

5. Parameters

The parameters of this model are derived from experiments done over cells [8, 10, 18].

In these experiments the authors measured the membrane tension and bending modulus in living cells, such as fibroblasts and erythrocytes. The measured parameters refer to the the cell plasmic membrane (i.e. the lipid bilayer) in combination with the actin cortex, which corresponds to the subdomain Ω_s. Using the theory of thin shells, we obtain the Lamé coefficients from the bending modulus and membrane tension. Other parameters in the model (cytoplasm viscosity or mass density) have been estimated from direct experiments on tissues.

TABLE 1. Parameters

Parameter	Range	Unit	Value used
ρ_f, fluid density	1	$\mathrm{Kg.L}^{-1}$	1
η, cytoplasm viscosity	1 to 250	Pa.s	10
L, domain length	3-5	μm	4
λ, membrane tension	$4.8\,10^{-6}$ to $3.6\,10^{-5}$	$\mathrm{J.m}^{-2}$	5.10^{-6}
k_b, bending modulus	10^{-20} to 10^{-19}	J	5.10^{-20}
A, force amplitude	1 to 10	nN	5

6. Numerical simulations and results

The resulting displacement field for the membrane-actin cortex, $\|\mathbf{W}\|$, is presented in Figure 9 whereas the cytoplasmic velocity field, $\|\mathbf{u}\|$, is shown in Figure 8. The mesh deformation, as well as the mesh velocity, $\|\mathbf{\Psi}\|$, are presented, respectively, in figures 10(a) and 10(b). As shown in figures 8 and 9, membrane bulging is small and shallow. This is representative of the situation where the membrane elasticity exerts a force which counterpoises the actin-driven force. The membrane's deformation increases in time until it reaches a mechanical equilibrium that stabilizes the domains' configuration. At equilibrium, the final configuration has the smallest possible curvature.

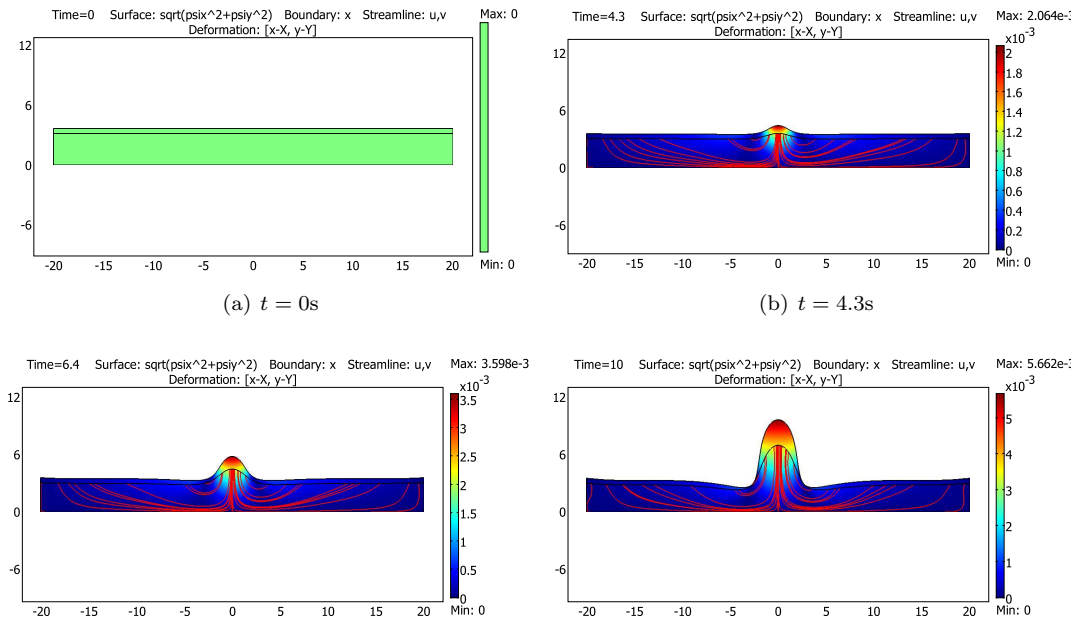

(a) $t = 0$s (b) $t = 4.3$s

(c) $t = 6.4$s (d) $t = 10$s

FIGURE 7. Deformation of the membrane and starting emergence of the filopodium.

To generate long and thin protrusion, one can modify the assumption that the cell material has constant mechanical properties as the actin-driven force develops. The figure 11 shows the cortex displacement that corresponds to the filopodium formation. In figure 11 we show the fluid velocity streamline and the

fluid velocity distribution when one assumes that the Young modulus of the cortex decreases with time. The final configuration looks like the observed nascent filopodium in actual cells [17].

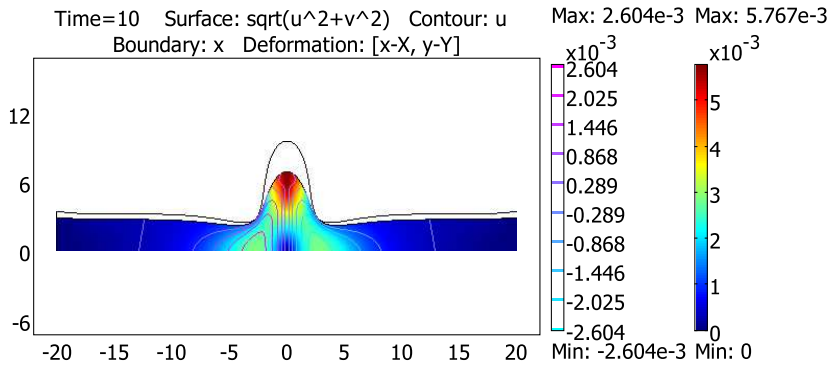

FIGURE 8. Deformation of the solid domain. Distribution of the cytoplasmic velocity $\|\mathbf{u}\|$ after application of a force at the actin-cortex/cytoplasm boundary.

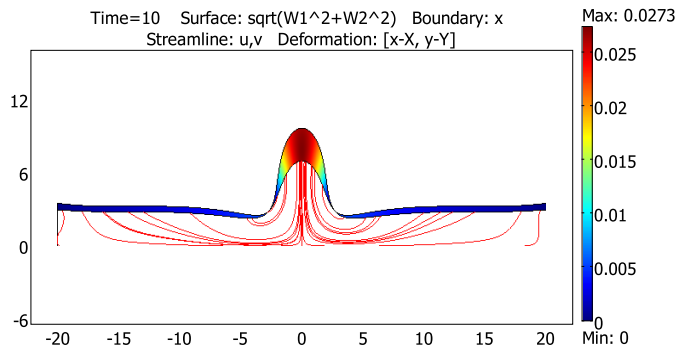

FIGURE 9. Formation of the filopodium (deformation of the solid domain). Distribution of the membrane's deformation stress. Streamlines of the cytoplasmic velocity $\|\mathbf{u}\|$.

7. Conclusion

This paper is devoted to the qualitative study of the fluid-structure interaction between the cytoplasm and the cell membrane in a 2D geometry. The cytoplasm is considered as a fluid and is described by Navier-Stokes equations. The cell membrane is modeled as a linear elastic material and is described by Navier equations. The parameters describing either the cytoplasm or the membrane and their behavior are taken from the literature and come from experimental data. The features of interest are the formation of the filopodia and the deformation of the domains of computation.

The use of the FSI modeling enabled to simulate the time-dependent distribution of stresses and strains developing within a cell membrane.

As an additional remark, we can say that, in this work, we presented a visco-elastic model, and we

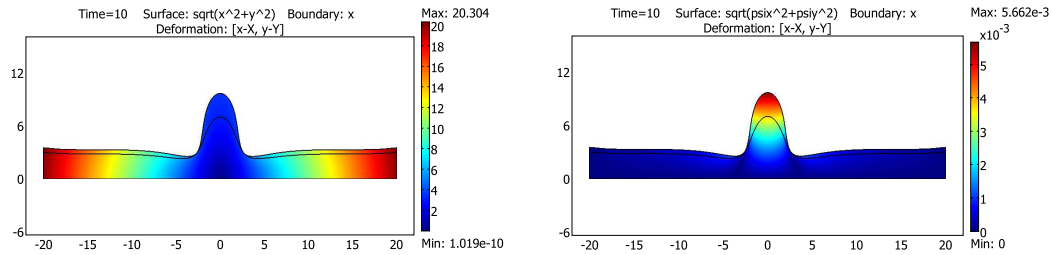

(a) Mesh displacement distribution.

(b) Mesh velocity distribution.

FIGURE 10. Mesh displacement and velocity.

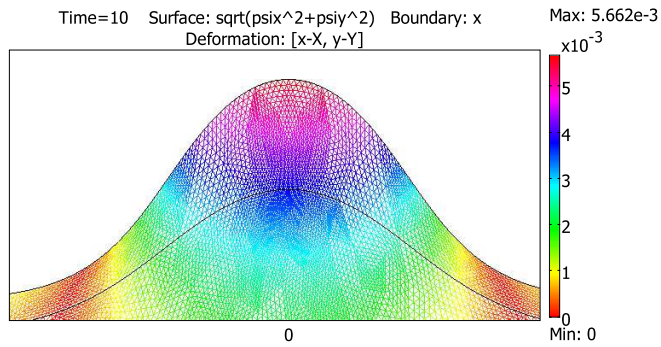

FIGURE 11. Zoom on the interface and display of the mesh velocity distribution showing the adaptive mesh chosen in order to perform numerical simulations.

consider the cytoplasm as a Newtonian fluid, that is a fluid with a constant viscosity. However it is more realistic to consider the cytoplasm as a Non-Newtonian fluid i.e. a fluid with a variable viscosity. A FSI model with a Non-Newtonian fluid is currently under development. Thus, we will be able to compare both Newtonian and Non-Newtonian effects on the development of the filopodia.

References

[1] B. Alberts, A. Johnson, J. Lewis J. Molecular Biology of the Cell (4th ed.). Garland Science. New York, 2002.

[2] F. Xue, D. M. Janzen, D. A. Knecht. *Contribution of Filopodia to Cell Migration: A Mechanical Link between Protrusion and Contraction*. International Journal of Cell Biology, vol. 2010, Article ID 507821, 13 pages, 2010.

[3] I. Budin, N.K. Devaraj. *Membrane Assembly Driven by a Biomimetic Coupling Reaction*. Journal of the American Chemical Society 134 (2), (2011), 751-753.

[4] Alberts JB, Odell GM *In Silico Reconstitution of Listeria Propulsion Exhibits Nano-Saltation*. PLoS Biol 2(12): e412 (2004), 2054-2066.

[5] D. Boal. Mechanics of the cell. Cambridge University Press, 2002.

[6] Nicolas Huc. Modèle pour l'étude du rôle de la membrane dans la dformation cellulaire : application à la spinogénèse. Université de Grenoble, 2004.

[7] N. El-Khatib, N. Huc, Y. Goldberg, J-L Martiel. *Analysis of Cell deformation with FEMLAB*. Proceedings of the COMSOL Multiphysics User's Conference, Paris 2005.

[8] E. Evans, R. Skalak. Mechanics and thermodynamics of biomembranes. CRC Press (1980).

[9] F. Gerbal, P. Chatin, Y. Rabin, J. Prost. *An elastic analysis of Listeria monocytogenes propulsion*. Biophysical J., 79, (2000), 2259-2275.

[10] S. Hénon, G. Lenormand, A. Richert, F. Gallet *A new determination of the shear modulus of the human erythrocyte membrane using optical tweezers*. Biophysical J., 76, (1999), 1145-1151.

[11] W.C. Hwang, R.E. Waugh. *Energy of dissociation of lipid from the membrane skeleton of red blood cells*. Biophysical J., 72, (1997), 2669-2678.

[12] G. Lenormand, S. Hénon, A. Richert, J. Siméon, F. Gallet *Direct measurement of the area expansion and shear moduli of the human red blood cell membrane skeleton*. Biophysical J. 81, (2001), 43-56.

[13] A. Mogilner, G. Oster*Cell motility driven by actin polymerization*. Biophysical J., 71, (1996), 3030-3045.

[14] A. Mogilner, L. Edelstein-Keshet *Regulation of actin dynamics in rapidly moving cells: A quantitative analysis*. Biophysical J., 83, (2002), 1237-1258.

[15] D. Needham, R.M. Hochmuth. *A sensitive measure of surface stress in the resting neutrophil*. Biophysical J., 61, (1992), 1664-1670.

[16] T. Pollard, G. Borisy. *Cellular motility driven by assembly and disassembly of actin filaments*. Cell, 112, (2003), 453-465.

[17] T.M. Svitkina, E.A. Bulanova, O.Y. Chaga, D.M. Vignjevic, S. Kojima, J.M. Vasiliev, G. Borisy. *Mechanism of filopodia initiation by reorganization of a dendritic network*. J. Cell. Biol.,160, (2003), 409-421.

[18] R. E. Waugh, R. G. Bauserman. *Physical measurements of bilayer-skeletal separation forces*. Ann. Biomed. Eng. 23, 1995, 308-321

[19] F. Nobile. *Numerical Approximation of Fluid- Structure Interaction Problems with Aplication to Haemodynamics*. PhD thesis, 2001.

[20] J. Janela, A. Moura, A. Sequeira. *A 3D non- Newtonian fluid-structure interaction model for blood flow in arteries*. Journal of Computational and Applied Mathematics, 234, 2010, 2783-2791.

[21] L. Formaggia, A. Moura, F. Nobile. *On the stability of the coupling of 3D and 1D fluid-structure interaction models for blood flow simulations*. ESAIM: Mathematical Modelling and Numerical Analysis, 41, 2007, 743-769.

[22] A. Chambolle, B. Desjardins, M. Esteban, C. Grandmont. *Existence of weak solutions for the unsteady interaction of a viscous fluid with an elastic plate*. J. Math. Fluid Mech., 7, 2005, 368-404.

[23] H. Beirão da Veiga. *On the existence of strong solutions to a coupled fluid-structure evolution problem*. J. Math. Fluid Mech., 6, 2004, 21-52.

[24] D. Coutand, S. Shkoller. *The interaction between quasilinear elastodynamics and the Navier-Stokes equations*. Arch. Ration. Mech. Anal. 179, 2006, 303-352.

[25] T.J.R. Hughes, W.K. Liu, T.K. Zimmermann. *Arbitrary lagrangian-eulerian finite element formulation for incompressible viscous flows*. Computer Methods in Applied Mechanics and Engineering, 29, 1981, 329-349.

[26] M. À. Fernández, M. Moubachir *A Newton method using exact jacobians for solving fluid-structure coupling*. Computers and Structures, v.83, 2005, 127-142.